

Interferometer Observations of Subparsec-scale Infrared Emission in the Nucleus of NGC 4151

M. Swain¹, G. Vasisht¹, R. Akeson², J. Monnier³, R. Millan-Gabet², E. Serabyn¹,
M. Creech-Eakman¹, G. van Belle², J. Beletic⁴, C. Beichman¹, A. Boden², A. Booth¹,
M. Colavita¹, J. Gathright⁴, M. Hrynevych⁴, C. Koresko², D. Le Mignant⁴, R. Ligon¹,
B. Mennesson¹, C. Neyman⁴, A. Sargent², M. Shao¹, R. Thompson¹, S. Unwin¹,
P. Wizinowich⁴

ABSTRACT

We report novel, high-angular resolution interferometric measurements that imply the near-infrared nuclear emission in NGC 4151 is unexpectedly compact. We have observed the nucleus of NGC 4151 at 2.2 μm using the two 10-meter Keck telescopes as an interferometer and find a marginally resolved source ≤ 0.1 pc in diameter. Our measurements rule out models in which a majority of the K band nuclear emission is produced on scales larger than this size. The interpretation of our measurement most consistent with other observations is that the emission mainly originates directly in the central accretion disk. This implies that AGN unification models invoking hot, optically thick dust may not be applicable to NGC 4151.

Subject headings: instrumentation: interferometers – galaxies: individual(NGC 4151) – galaxies: Seyfert

1. Introduction

NGC 4151 is the nearest and brightest Seyfert and it has been identified as the “archetype” of Seyfert 1 galaxies (Neugebauer, Graham, Soifer, & Matthews 1990). It has also been called “one of the most enigmatic” of galaxies (Cassidy & Raine 1996) because the origin of the

¹Jet Propulsion Laboratory, California Institute of Technology, 4800 Oak Grove Dr., Pasadena, CA 91109

²Michelson Science Center, California Institute of Technology, 770 S. Wilson Ave., Pasadena, CA 91125

³Univ. of Michigan, 941 Dennison Bldg, Ann Arbor, MI, 48109

⁴W. M. Keck Observatory, California Association for Research in Astronomy, 65-1120 Mamalahoa Hwy., Kamuela, HI 96743

near-infrared nuclear emission component, which dominates galactic near-infrared emission, is unclear. The extent to which the observed near-infrared emission comes directly from the accretion disk or jet rather than from clouds of gas or dust that *reprocess* energy from the accretion disk is critical to models that attempt to unify various observational classes of AGN (Antonucci 1993). Over the past 30 years, arguments for both thermal and nonthermal (synchrotron) emission mechanisms have been proposed (see Neugebauer, Graham, Soifer, & Matthews (1990) and references therein). Evidence of *K* band emission variability on 1–2 month timescales (Penston et al. 1974; Rieke & Lebofsky 1981; Oknyanskij et al. 1999) and weak (0.1–0.5%) degrees of *H* and *K* band linear polarization (Kemp et al. 1977; Ruiz et al. 2003) can be explained by both thermal and nonthermal models. Currently, the prevailing view is that the near-infrared emission is thermal and arises from the inner edge of a dust torus that is heated primarily by UV and soft x-ray emission from the corona of the accretion disk surrounding a massive black hole (Antonucci 1993). In this picture, the source of the near-infrared emission would appear spatially unresolved by the largest single aperture infrared telescopes and would have low degrees of linear polarization.

Observations at 11 μm (Neugebauer, Graham, Soifer, & Matthews 1990; Radomski et al. 2003) strongly imply the presence of a <35 pc diameter source where dust grains are heated to around 200 K and are responsible for the mid-infrared emission. Estimates for the inner radius of the dust, which could correspond to the inner edge of a torus, have been as small as about 0.03 pc (Rieke & Lebofsky 1981), with values in the 0.2–1 pc range presently favored (Antonucci 1993; Pier & Krolik 1992; Evans et al. 1993; Ruiz et al. 2003). In some AGN unification schemes, the torus is supposed to be optically and physically thick (Antonucci 1993). The radius of the broad line region (BLR) is about 0.01 pc (Clavel et al. 1990), putting the smallest estimates of the dust torus’ inner radius very close to the black hole and accretion disk.

The parent galaxy for the NGC 4151 Seyfert nucleus is nearly face-on ($i = 21^\circ$ to the line of sight) and has a weak radio jet at P.A. = 77° E. of N. (Mundell, Wrobel, Pedlar, & Gallimore 2003). While the radio feature corresponding to the UV/optical nucleus has been uncertain, the candidate features contain emission knots that are unresolved on angular scales of a few milliarcseconds (mas) and have a surface brightnesses of a few mJy/beam (Mundell, Wrobel, Pedlar, & Gallimore 2003; Ulvestad, Roy, Colbert, & Wilson 1998). The 2MASS *K* band flux for NGC 4151 is 8.519 ± 0.018 magnitudes, and at least 90% of the flux is contained in the central 1 arcsec (Kemp et al. 1977). The bolometric luminosity of the AGN is about 10^{44} erg s^{-1} , and a $10^7 M_\odot$ black hole is thought to lie at the center of the BLR (Ulrich 2000). Following Mundell, Wrobel, Pedlar, & Gallimore (2003), we have taken the distance as 13.3 Mpc (for $H_0 = 75$ km s^{-1}), where 1 mas corresponds to 0.065 pc (75.3 light days) in projection.

Interferometric combination of the twin Keck telescopes (Colavita & Wizinowich 2002) provides sensitivity to $2.2 \mu\text{m}$ emission on angular scales of ~ 1 mas. Our observations represent a ten-fold improvement in angular resolution when compared to previous near-infrared measurements of AGN and make it possible to test the subparsec-scale, near-infrared emission models of NGC 4151. Optical/IR interferometry has traditionally been limited to relatively bright stellar objects. These observations represent the first measurement of an extragalactic source with an optical/IR interferometer.

2. Observations and Data Reduction

2.1. Observations

The Keck Interferometer combines the light from the two 10 m Keck telescopes, separated by 85 m with the baseline oriented 38° (E of N). Both telescopes are equipped with adaptive optics systems (Wizinowich et al. 2002), which are required for K band interferometer observations. The interferometer field of view on the sky is ~ 50 mas in the K band, as set by a single-mode fiber ahead of the detector; the interferometer is not sensitive to emission outside of this field of view. The fringe tracker uses a 4-bin synchronous fringe demodulation algorithm (Vasisht et al. 2002), similar to that used at the Palomar Testbed Interferometer (Colavita et al. 1999). For the data presented here, the system operated at a 200 Hz frame rate (the 4-bin acquisition time).

NGC 4151 was observed with the Keck Interferometer on 2003 May 20 and 21. The data presented here are from the white-light channel ($\lambda_{\text{center}}=2.18 \mu\text{m}$ and $\Delta\lambda \sim 0.3\mu\text{m}$). Observations consist of a series of interleaved integrations on the source and several calibrators. Each integration includes 120 seconds of fringe data followed by a background measurement. Included with the fringe data are periodic measurements of the single-telescope fluxes. The data are presented as the visibility amplitude squared, normalized such that an unresolved object has $V^2 = 1.0$. On May 20, only limited data were collected on NGC 4151 and calibrators due to weather; however, the source was detected and resolved on both nights, with internally consistent visibility. In the results discussed below we have used data only from May 21.

2.2. Data Reduction

The system visibility, the instrument response to a point source, is measured with respect to the calibrator stars HIP58918, HD 105925, and HIP60286. The calibrator angular sizes

were derived by fitting photometry from SIMBAD and 2MASS. All of the calibrators have estimated angular diameters of less than 0.2 mas and are unresolved by the interferometer. The calibrator angular size uncertainty was set to 0.1 mas. Source and calibrator data were corrected for biases using sky calibrations as described by Colavita (1999) and averaged into blocks of 5 seconds each. The calibration procedure includes a per-scan correction for the bias due to mismatched fluxes between the two telescopes (which includes Strehl mismatch) using the single-telescope flux measurements.

The data were then calibrated for the system visibility (Boden et al. 1998). The calibrated data points for the target source are the average of the 5 seconds blocks in each integration, with an uncertainty given by the quadrature of the internal scatter and the uncertainty in the calibrator size. In addition to the measurement error, we have estimated any systematic error in the calibrated visibility to be less than 0.05 (Colavita et al. 2003). This systematic error was summed quadratically with the measurement and calibration errors. The resulting average visibility is 0.84 ± 0.06 at an average projected baseline of 82.7 m at a P.A. = 37° E of N. The calibrated visibilities and the system visibility estimates are shown in Fig. 1.

3. Discussion

3.1. Compact Emission

If all the light in the fringe tracker field of view (approximately the diffraction limit of the single telescope) came from an unresolved point source, the interferometer calibrated V^2 would be unity. Our measured V^2 is relatively high, implying the source of this emission is small. A variety of compact flux distributions could produce the measured visibility; we have used three simple, geometric models to estimate the angular size of the emission. The models correspond to a “face-on” inclination and are constrained to fit the measured V^2 . If the emission is distributed as a single-component Gaussian, the FWHM = $0.98 \text{ mas} \pm 0.18 \text{ mas}$. If the the emission is distributed as a ring, the ring inner diameter = $0.96 \text{ mas} \pm 0.26$ with a width = 0.06 mas , where the width is set to match the total K band flux for an optically thick medium with a temperature of 1500 k. If the emission is distributed as a point source with an extended (over-resolved) component, the point-source fraction of the flux = 0.92 ± 0.04 of the flux. Whatever the details of the emission distribution or mechanism, the bulk of the emission comes from a compact ($\leq 1.52 \text{ mas}$ at the 3σ level) region. Our measurements rule out any scenario with a majority of the K band nuclear emission coming from a region with a radius in projection larger than 0.05 pc.

3.2. Possible Emission Mechanisms

We consider four possible mechanisms for the K band emission. Because of the combined constraints implied by our measurement and other observations, we find two of the cases to be unlikely.

Synchrotron Emission: VLBA imaging of NGC 4151 at a few mas scales (Ulvestad, Roy, Colbert, & Wilson 1998) reveals that its parsec-scale radio jet is subluminoous; it is several orders of magnitude fainter than the parsec-scale radio jets imaged in nearby classical radio galaxies. Measurements at 18 cm and 6 cm of the nuclear region reveal a relatively flat spectrum (ν^α with $\alpha \simeq -0.3$) source with a peak flux density of about 1 mJy mas^{-2} . In contrast, the large near-infrared flux density of $\simeq 10^2 \text{ mJy mas}^{-2}$ is inconsistent with the radio fluxes and implies that the nuclear near-infrared source is unrelated to the radio source and, by inference, unrelated to a subparsec-scale synchrotron jet.

Star Cluster: Explaining the compact K band emission as stellar would require $\sim 3 \times 10^6$ O stars in a volume of $\sim 0.001 \text{ pc}^3$. This explanation is unlikely, as it would imply a density for young stars $\sim 100,000$ times higher than in our own galactic center (Morris & Serabyn 1996; Genzel et al. 2000). A stellar component is also incompatible with the measured infrared intensity fluctuations (Rieke & Lebofsky 1981; Quillen et al. 2000).

Thermal Dust: If the dust is distributed as a physically thick torus, the inner radius is much smaller than typically estimated. The smallest possible scale for thermal dust emission is set by the dust sublimation radius. Using the model of Barvainis (1987), we find dust with a temperature of 1900 K, corresponding to a sublimation radius of 0.05 pc, is consistent with our measurement. Thus, if the infrared emission is from centrally heated dust, it is consistent with our observations only if the dust is very hot and the K band emission is localized near the dust sublimation radius.

Thermal Gas: A simple, face-on, geometrically thin accretion disk model, with $T \propto r^{-3/4}$ (Shakura & Sunyaev 1973) and with an inner temperature of $\sim 3.5 \times 10^5 \text{ K}$ (consistent with the soft x-ray emission (Ulrich 2000)), predicts a K band magnitude of 8.4, 95% of which is inside a radius of $\sim 0.01 \text{ pc}$. This model predicts an unresolved point source, consistent with our size measurement and with approximately the measured near-infrared flux.

Both the thermal dust and thermal gas models are consistent with our observations. However, centrally heated dust, which is thought to reprocess UV/optical radiation from the central engine, produces a specific signature known as the “infrared bump” (Barvainis 1987; Sanders et al. 1989). There is no evidence for a comparable feature in NGC 4151 (Rieke & Lebofsky 1981; Edelson & Malkan 1986; Alonso-Herrero et al. 2001). Also, a dust torus with a well-defined, but small, inner radius (corresponding to the sublimation radius) would give

similar time delays between fluctuations in the UV/optical flux and fluctuations in the H and K band flux. This is inconsistent with the analysis by Oknyanskij et al. (1999). Thus the absence of the “infrared bump” and the presence of the H/K time delay difference both support the interpretation that the bulk of the infrared flux measured with the interferometer arises from an unresolved accretion disk.

4. Summary and Conclusions

We have measured the angular diameter of the K band emission in the nucleus of NGC 4151. Our observations rule out any emission mechanism that requires a large fraction of the nuclear K band emission to be produced at a radius of greater than 0.05 pc from the black hole. Taken in the context of other observations, we interpret our measurement as evidence that a majority of the K band emission comes from a central accretion disk.

We dedicate these observations to the memory of Jim Kelley, the late project manager and tireless advocate of the Keck Interferometer. We thank Robert Antonucci, Roger Blandford, and Julian Krolik for useful discussions. The Keck Interferometer is funded by the National Aeronautics and Space Administration as part of its Navigator program. Part of this work was performed at the Jet Propulsion Laboratory, the California Institute of Technology, and the Michelson Science Center, under contract with NASA. Observations presented were obtained at the W.M. Keck Observatory, which is operated as a scientific partnership among the California Institute of Technology, the University of California, and NASA. The authors wish to recognize and acknowledge the very significant cultural role and reverence that the summit of Mauna Kea has within the indigenous Hawaiian community. We are most fortunate to have the opportunity to conduct observations from this mountain. The Observatory was made possible by the generous financial support of the W.M. Keck Foundation. This work has made use of software produced by the Michelson Science Center at the California Institute of Technology. This work has also made use of the SIMBAD database, operated at CDS, Strasbourg, France, and the NASA/IPAC Infrared Science Archive, operated by the JPL under contract with NASA.

REFERENCES

- Alonso-Herrero, A., Quillen, A. C., Simpson, C., Efstathiou, A., & Ward, M. J. 2001, *AJ*, 121, 1369

- Antonucci, R. 1993, *ARA&A*, 31, 473
- Barvainis, R. 1987, *ApJ*, 320, 537
- Boden, A. F., Colavita, M. M., van Belle, G. T., & Shao, M. 1998, *Proc. SPIE*, 3350, 872
- Cassidy, I. & Raine, D. J. 1996, *A&A*, 310, 49
- Clavel, J. et al. 1990, *MNRAS*, 246, 668
- Colavita, M. M., et al., *ApJ*, submitted
- Colavita, M. M. 1999, *PASP*, 111, 111
- Colavita, M. M. et al. 1999, *ApJ*, 510, 505
- Colavita, M. M. & Wizinowich, P. L. 2002, *Proc. SPIE*, 4838, 79
- Edelson, R. A. & Malkan, M. A. 1986, *ApJ*, 308, 59
- Evans, I. N., Tsvetanov, Z., Kriss, G. A., Ford, H. C., Caganoff, S., & Koratkar, A. P. 1993, *ApJ*, 417, 82
- Genzel, R., Pichon, C., Eckart, A., Gerhard, O. E., & Ott, T. 2000, *MNRAS*, 317, 348
- Kemp, J. C, Rieke, G. H., Lebofsky, M. J, & Coyne, G. V. 1977, *ApJ*, 215, L107
- Morris, M. & Serabyn, E. 1996, *ARA&A*, 34, 645
- Mundell, C. G., Wrobel, J. M., Pedlar, A., & Gallimore, J. F. 2003, *ApJ*, 583, 192
- Neugebauer, G., Graham, J. R., Soifer, B. T., & Matthews, K. 1990, *AJ*, 99, 1456
- Oknyanskij, V. M., Lyuty, V. M., Taranova, O. G., & Shenavrin V. I. 1999, *AL*, 8, 563
- Penston, M. V., Penston, M. J., Selmes, R. A., Becklin, E. E., & Neugebauer, G. 1974, *MNRAS*, 169, 357
- Pier, E. A., & Krolik, J. H. 1992, *ApJ*, 401, 99
- Quillen, A. C., Shaked, S., Alonso-Herrero, A., McDonald, C., Lee, A., Rieke, M. J., & Rieke, G. H. 2000, *ApJ*, 532, L17
- Radomski, J. T., Piña, R. K., Packham, C., Telesco, C. M., De Buizer, J. M., Fisher, R. S., & Robinson, A. 2003, *ApJ*, 587, 117

- Rieke, G. H., & Lebofsky, M. J. 1981, *ApJ*, 250, 87
- Ruiz, M., Young, S., Packham, C., Alexander, D. M., & Hough, J. H. 2003, *MNRAS*, 340, 733
- Sanders, D. B., Phinney, E. S., Neugebauer, G., Soifer, B. T., & Matthews, K. 1989, *ApJ*, 347, 2
- Shakura, N. I. & Sunyaev, R. A. 1973, *A&A*, 24, 337
- Ulrich, M.-H. 2000, *A&A Rev.*, 10, 135
- Ulvestad, J. S., Roy, A. L., Colbert, E. J. M., & Wilson, A. S. 1998, *ApJ*, 496, 196
- Vasisht, G., Booth, A., Colavita, M. M., Johnson, R. L., Ligon, E. R., Moore, J. D. & Palmer, D. L. 2002, *Proc. SPIE*, 4838, 824
- Wizinowich, P., Le Mignant, D., Stomski, P., Acton, D.S., Contos, A., & Neyman, C., 2002, *Proc. SPIE*, 4839, 9

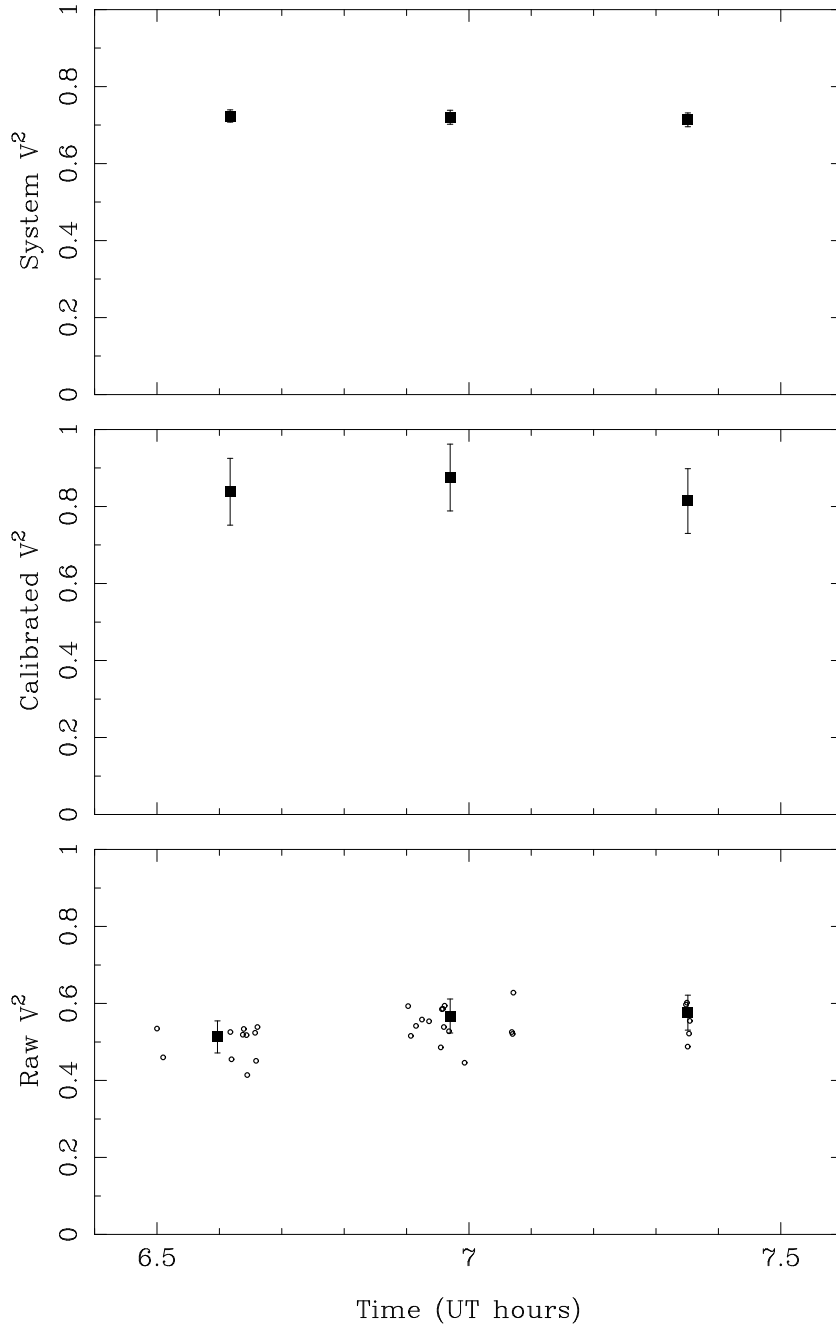


Fig. 1.— The raw (bottom), calibrated (middle) and system visibility (top) for NGC4151. In the raw data plot, the 5 sec data averages are shown with open circles and the scan averages are shown with filled squares. The measured visibility is 0.84 ± 0.064 ; the error bars in the calibrated data contain a 5% systematic component. The hour angles for the averaged points are -0.03, 0.33 and 0.71 hours respectively. The projected baseline length ranges from 81.8 to 83.6 meters and the position angle from 39.3 to 33.9 degrees (E of N).